Journal of Solar Energy Research (JSER)

Journal homepage: www.jser.ut.ac.ir

Development of a novel film condensation-based heat transfer model to estimate the productivity of conventional solar still

Ram Kumar[a*], Dhananjay R. Mishra[a], Pankaj Dumka[a]

[a] *Department of Mechanical Engineering, Jaypee University of Engineering and Technology, A.B. Road, Guna - 473226, Madhya Pradesh (India).*

ARTICLE INFO

Article Type:

Research Article

Received:14.10.2024
Accepted:26.02.2025

Keywords:
Desalination;
Conventional solar still;
Film condensation;
Predictive model;
Heat transfer

A B S T R A C T

This manuscript describes the development of a film condensation model based on heat and mass transfer principles. The objective of the model is to estimate the amount of distillate yield derived from CSS. To verify the accuracy and effectiveness of the proposed model, experiments were performed on CSS, and the results were compared with theoretical predictions derived from the model. Moreover, a well-established Dunkle model has also been applied to check the prediction strength of the proposed theory. The observation shows that the proposed model provides a prediction for the distillate output that is substantively close to the experimental result with a deviation of only 4.0%, whereas the overall distillate yield estimated from Dunkle's model shows a significantly higher deviation of 116.8%. These results underscore the superior accuracy and reliability of the proposed film condensation-based heat transfer model, especially in comparison to the Dunkle model, in predicting the performance and distillate output of passive solar stills.

1. Introduction

Water, which is an essential resource for the existence of human beings on the earth, is perishing day by day. The major causes of water scarcity are rapidly growing industries and population. The irony of the situation is that two-thirds of the water surrounds us, but the majority of the world is facing water crises. This has compelled people to live in scarcity of potable water, resulting in malnutrition in the younger generation. The vast majority of water on our planet is either salty or brackish; hence, it can't be consumed

*Corresponding Author Email: ram.baghel18 @gmail.com

Cite this article: Kumar, R. , Mishra, D. R. and Dumka, P. (2024). Development of a novel film condensation-based heat transfer model to estimate the productivity of conventional solar still. Journal of Solar Energy Research, 9(4), 2102-2114. doi: 10.22059/jser.2025.383742.1481

DOI: 10.22059/jser.2025.383742.1481

in its current form. So, to cater to the needs of the growing population, researchers are diligently working on developing new technologies and improving existing ones that can transform seawater into potable water. The techniques that are commonly employed for producing portable water are very energy-intensive and, hence, can't be used by underdeveloped countries. So, researchers have shifted their attention towards sustainable and eco-friendly methods instead of relying on fossil fuel-based technologies in order to develop water treatment solutions. Solar energy represents a perpetual, environmentally friendly, and sustainable source that can be utilized to address water scarcity issues. An apparatus commonly known as conventional solar still utilizes solar energy to transform seawater into potable water. CSS works on green-house theory, and it is straightforward to handle. Though solar desalination has a history of more than 500 years the first instance of the use of CSS is seen in the work of Carlos Wilson [1]. The downsides of CSS are its low productivity and the requirement of substantive surface area to capture solar radiation and facilitate evaporation. Therefore, several modifications have been suggested by many researchers to improve the productivity of CSS. Kabeel and El-Agouz [2] have examined the progress and innovations in solar energy-based desalination systems. Similarly, Ayoub and Malaeb [3] analyzed the latest developments in this field. Prakash and Velmurugan [4] comprehensively explored the key factors affecting the efficiency of solar desalination systems. Panchal and Mohan [5] extensively discussed different approaches for boosting the distillate yield of solar-powered water purification systems. Likewise, Panchal et al. [6] reviewed multiple strategies for raising the distillate production of enhanced solar still systems. In their comprehensive review, Mevada et al. [7] have extensively examined how fin design parameters affect the efficacy of solar-powered desalination systems. Panchal et al. [8] conducted an in-depth review on the application of distinct thermal storage materials and their effects on the efficacy of desalination systems.

Tiwari & Tiwari [9] studied the correlation between the water depth and the productivity of solar distiller units. The impact of varying aspect ratios on the performance of CSS has been studied by Jamil and Akhtar [10]. Afrand and Karimpour [11] have documented the influence of weather conditions on the efficacy of conventional desalination units. Dumka and Mishra [12] explored how changes in salt concentrations affect the performance of CSS. A comparative study on the performance characteristics of conventional and earth stills has been conducted by Dumka & Mishra [13,14]. The impact of carbon-infused foam and bubble wrap on the efficacy of CSS has been examined by Arunkumar et al. [15]. Whereas, the yield of CSS enriched with organic and inorganic PCM (Phase Change Materials) has been investigated by Kabeel et al. [16]. Moreover, Kabeel et al. [17] have also examined the influence of jute-wrapped sand on the performance of CSS. Mishra and Tiwari [18] reported the enhanced yield of CSS using metal chips. Khanafer and Vafai [19] conducted a comprehensive analysis of the performance of CSS augmented with nano-fluids, as reported in their extensive review. Deshmukh and Thombre [20] have advocated the adoption of a sensible energy storage medium (servo-therm oil) to elevate the efficiency of CSS. Dumka et al. [21] performed experiments to reduce the surface tension of water by using permanent ferrite ring magnets. They noticed a significant enhancement of 49.2% in the distillate yield due to the magnetization effect. To introduce turbulence in the basin water, solar-powered stirrers and wind-driven water fans were documented by Rajaseenivasan et al. [22] and Omara et al. [23], respectively. Kabeel et al. [24] have used TiO2 coating with black paint to eliminate the need for a medium for storing energy. To augment both the surface area and turbulence within the basin water, Dumka & Mishra [25] have documented the utilization of an ultrasonic fogger in the basin. A comparative analysis of conventional and honeycomb pad-augmented solar stills has been performed by Kumar et al. [26]. Dumka et al. [27] documented an experimental study on a conventional solar still enhanced with saltwater bottles. Their modifications led to a 20% reduction in the cost of yield compared to the conventional solar still (CSS).

Shoeibi et al. [28] investigated the methodologies, characteristics, and components involved in the encapsulation process, assessing the influence of encapsulated PCM formulations on the efficiency of various solar energy technologies. Their study covered applications such as photovoltaic systems, solar desalination units, solar power plants, solar ponds, thermochemical reactors, and related technologies. Moreover, Shoeibi et al. [29] have comprehensively examined various methods aimed at improving the condensation rate in solar desalination systems. Hemmatian et al. [30] conducted an experimental and environmental study aimed at improving the performance of solar stills by

incorporating thermal pipe and pulsating thermal pipe vacuum tube solar absorbers along with phase change materials (PCM) for latent heat storage. Their findings indicated that solar stills utilizing thermal pipes achieved an energy efficiency of 19.4%, while those equipped with pulsating thermal pipes exhibited a slightly higher efficiency of 20.3%. Khalili et al. [31] conducted an experimental study on an HDH desalination unit powered by a CGS gas heater incorporating thermosyphon thermal pipes. Their findings indicated that the highest energy and exergy efficiencies were obtained when the airspeed was set to 0.6 m/s. Dhivagar et al. [32] investigated the impact of incorporating crushed granite rock in solar-powered desalination systems integrated with solar district heating. Their study revealed an enhancement in energy efficiency and an increase in exergy efficiency at a water depth of 1 cm compared to greater depths of 2 cm and 3 cm. Abdelmaksoud [33] conducted an experimental study to analyze the impact of combining solar still with heat storage materials and a planar solar thermal collector on freshwater generation. He reported that in comparison to conventional still, CSS enhanced with heat storage material achieved an 11–32% increase in the daily productivity of pure water, while CSS incorporating both heat storage material and a solar collector demonstrated a significant 155–183% rise in daily pure water productivity.

Teles et al. [34] investigated the use of innovative solar collectors with reflective surfaces positioned in an eccentric arrangement to supply energy to absorption chillers and decrease the average cooling cost per unit. Their findings suggested that this advanced type of solar collector could enhance cost efficiency by 29%. Bhargva et al. [35] conducted an experimental investigation to enhance the efficiency of solar stills by incorporating rectangular fins and bamboo cotton wicks. Their findings indicated a 19% increase in daily distillate production. Farzi et al. [36] examined the effect of sand particle grain size on the distillate yield of passive solar stills. The results demonstrated that utilizing sand with an average grain size of 2.8 mm led to improved performance and higher thermal efficiency. Similarly, Gholizadeh et al. [37] enhanced the productivity of passive solar still by introducing sand into the basin, achieving a 21.16% increase in output. Ahmed et al. [38] reported a detailed review that critically analyzes design improvements and operational procedures to enhance the performance of solar stills. They noted that the use of PCMs, such as paraffin wax, can boost the productivity of solar stills by 87.4%, while the application of CuO nanofluids and revolving wick mechanisms results in an impressive 350% increase in the production of safe water. Alamshah et al. [39] examined variations in production rates in relation to solar energy intensity and saltwater pool temperature. According to their study, the thermal efficiency of the system was recorded at 27.1%, aligning with findings from similar research. Das and Date [40] investigated the combined use of residual heat energy and eductor systems, examining how eductor technology can be integrated with low-grade residual heat energy in desalination processes. Their research proposed a novel strategy to increase energy efficiency, reduce operational expenses, and mitigate environmental impact. El-Sayed M.Essa et al. [41] conducted a comprehensive and up-to-date review of solar desalination units, focusing on the integration of solar photovoltaic and thermal energy systems. The study explored recent advancements in solar desalination approaches, demonstrating how this integration enhanced energy efficiency.

To judge the efficacy of CSS numerically, several researchers have developed many theoretical models by utilizing principles of heat-mass transfer. Dunkle [42] was the first to develop a semi-empirical model based on the principle of heat-mass transfer. Later, Cooper [43,44] gave his own ranges of Grashof by working on the theory given by Dunkle. The Sankey diagram-based mathematical model for CSS has been formulated by Frick [45]. Nayak et al. [46] and Sodha et al. [47] have worked on transient and periodic analysis to estimate the distillate production of solar stills. Moreover, a better version of the time-dependent model for CSS has been reported by Kamal [48] for varying basin water and thickness of insulation. To estimate the values of both constants C and n, a linear regression model that incorporates heat-mass transfer principles has been reported by Kumar & Tiwari [49]. This model can predict a good result as it is independent of the Grashof number range. Moreover, Dumka and Mishra also reported a mathematical model based on regression for estimating the output of CSS. A Chilton-Colburn analogy-based numerical model to predict the productivity of conventional solar still has been developed by Tsilingiris [50]. Kiatsiriroat et al. [51] have documented a mass transfer-based model for estimating the distillate production of CSS, which is based on Spalding's mass transfer.

Existing literature indicates that significant endeavors have been attempted to escalate the

efficiency and distillation of solar stills. Moreover, multiple researchers have formulated heat-mass models for estimating the output of CSS, but no one has ever considered the condensation phenomenon for predicting the distillate yield. The cardinal objective of the current study is to devise a novel theoretical model centered around the condensation phenomenon. The model is based on the heat transfer aspect of condensation, and it is expected that it will perform better for any range of temperatures. Existing models, such as the Dunkle [42] and other heat-mass models [52–54], provide estimates of distillate output under various conditions but fail to account for the heat transfer associated with condensation, which affects the overall efficiency and yield of the system. The proposed model addresses this gap by incorporating the condensation rate into the theoretical framework, offering a more accurate prediction of distillate output. By focusing on the heat transfer during condensation, the model outperforms conventional models in terms of predictive accuracy, particularly in scenarios where temperature variations are significant.

While the suggested model gives a novel methodology for predicting the yield of CSS by incorporating the condensation phenomenon, certain limitations need to be acknowledged. The model assumes a uniform condensation behavior across the condensing surface, which may change in actual conditions due to the non-uniform temperature gradients and external climatic factors, viz., wind speed, humidity, and solar intensity fluctuations. Also, the applicability of this model to different CSS designs, such as stepped, pyramid, and multi-effect stills, remains an open research question. Future studies can confirm the model's robustness by testing its predictions under varying environmental conditions and for alternative CSS configurations. Likewise, integrating advanced computational techniques, such as machine learning or CFD simulations, could refine the model's predictive capability.

In addition to the limitations mentioned above, it is important to note that the applicability of the proposed model may be influenced by varying environmental conditions and the specific configuration of the CSS systems. The assumptions of constant solar irradiance and uniform heat transfer may not fully capture the complexities encountered in real-world scenarios, particularly in regions with highly variable weather patterns or larger, more intricate CSS configurations.

2. Experimental setup

The purpose of this experiment is to predict the mass of condensed film on the inside surface of the condensing cover made of clear glass by investigating the performance of conventional solar stills. For this purpose, a single slope, south facing, 1m^2 basin area, conventional solar still was fabricated from FRP material of thickness 5 mm at JUET, Guna. The heights of the upper and lower vertical walls are 48 and 20 cm, correspondingly. To improve the absorption of radiation, the interior surfaces within the apparatus were coated in black.

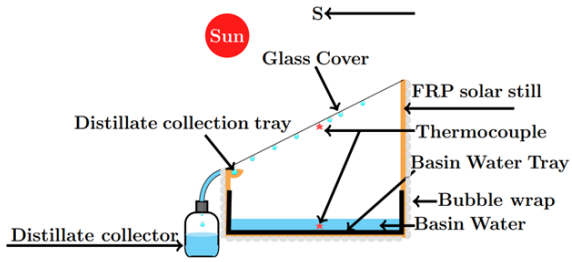

Figure 1. Schematic representation of CSS

A condensing surface, made of clear glass of 4 mm thickness, has been employed for covering the still at an altitude of 24° with respect to the earth's surface. Arunkumar et al. [15] employed bubble wrap as an insulating material to minimize thermal energy loss from the sides of the still. Figure 1 depicts the schematic arrangement of the conventional solar still. The entire experimental apparatus is depicted in Figure 2.

Five thermocouples were used to measure ambient, inner condensing cover, outer condensing cover, water surface, and basin temperatures. During the entire experiment, all temperatures were recorded using a temperature indicator (DTC324A-2), while a solar power meter (LX-107) was utilized to record the incoming solar energy on the condensing cover.

Several potential sources of error were present in the experimental setup, which may have influenced the accuracy of the results. These include uncertainties in the measurement of temperature and solar radiation due to the calibration of instruments and environmental fluctuations. Heat losses from the system, which were not fully accounted for, could also have impacted the results, as well as slight variations in the material properties of the CSS throughout the testing period. Furthermore, manual errors during data collection and potential misalignments of the solar stills may have contributed to discrepancies.

Type B uncertainties are incorporated into the experiments, assuming uniform data distribution. The computation of this type of uncertainty is done as [55]:

Figure 2. Photograph of experimental apparatus

$$u_1 = \frac{a_1}{\sqrt{3}} \quad (1)$$

where a_1 represents the equipment's accuracy. Information regarding the standard uncertainties of the measuring equipment is provided in Table 1.

Table 1. Accuracy, range and standard uncertainties of measuring devices

Equipment	Accuracy	Range	Standard Uncertainty
Solari meter (W/m^2)	±10	0 - 1999	5.77
Temperature probe (°C)	± 0.10	-100 500	0.06
Measuring cylinder (mL)	± 1	0 - 250	0.6

In April and May 2024, outdoor experiments were carried out at JUET, Guna (latitude: 24° 39′ N, longitude: 77° 19′ E), India. Each experimental run lasts for 24 h. The following findings were noted during the investigation:

- Ambient, inner and outer condensing cover, water surface, and basin temperatures,
- Level of incoming solar radiation on an inclined condensing cover,
- The output of distillates per hour.

3. Theoretical Background

3.1. Dunkle model

The combined internal heat transmission involves three distinct mechanisms: convective, evaporative, and radiative heat transfer. The internal heat transmission via the mode of convection is calculated as follows [1]:

$$\dot{q}_{cw} = h_{cw} \times \left(T_w - T_{ci}\right) \quad (2)$$

where, h_{cw} is computed using the Nusselt (Nu), Grashof (Gr), and Prandtl (Pr) number relation as [9]:

$$Nu = \left(\frac{h_{cw} \times d}{k}\right) = C \times \left(Gr \times Pr\right)^n \quad (3)$$

In order to calculate h_{cw} in Eqn. (3) it is necessary to have the values of C and n. The first time Dunkle [27] published the semi-empirical relations for the calculation of h_{cw} was in 1961. For different values of the Rayleigh number $(Ra = Gr \times Pr)$, he proposed C and n values. The model exhibits good predictive performance when the average temperature range is 50°C, and the operational temperature range is 17°C. To calculate the value of h_{cw}, this model proposed Eqn. (4) [42].

$$h_{cw} = 0.844\left(T_w - T_{ci} + \frac{(P_w - P_{ci})(T_w + 273)}{2.689 \times 10^5 - P_w}\right)^{\frac{1}{3}} \quad (4)$$

The value of h_{ew} is calculated after evaluating the value of h_{cw} as [42]:

$$h_{ew} = 0.016273 \times h_{cw} \times \left(\frac{P_w - P_{ci}}{T_w - T_{ci}}\right) \quad (5)$$

The theoretical distillate yield can, therefore, be computed as follows [1]:

$$\dot{m}_{ew} = \frac{\dot{q}_{ew} \times A_s \times 3600}{h_{fg}} = \frac{h_{ew} \times A_s \times 3600 \times \left(T_w - T_{ci}\right)}{h_{fg}} \quad (6)$$

3.2. Proposed theoretical model

In the desalination process, film forms on the inner condensing cover which trickles and rolls down the inclined surface due to gravitational effect. The thickness of the film and its flow rate escalate when it moves from top to down the glass surface due to ongoing condensation on the interface of liquid and vapour at saturation temperature T_{sat}. As $T_s < T_{sat}$. the transfer of heat energy from the interface of the liquid and vapour to the glass cover is maintained through the film. By using the assumptions that Brouwers [56] used in his work, thickness and mass flow rate may be calculated.

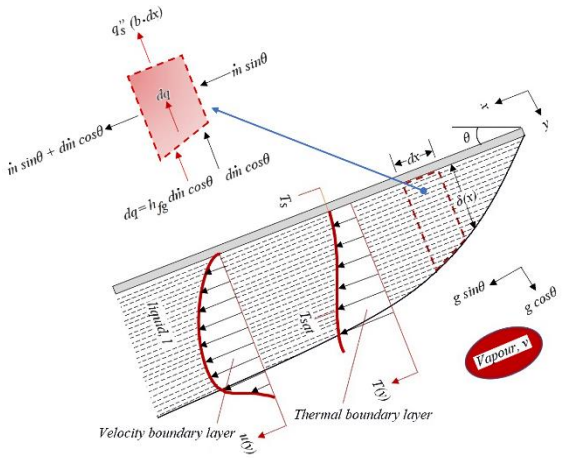

Figure 3. Boundary layer effects related to film condensation on an inclined plate

Figure 3 depicts the impact of boundary layer phenomena resulting from the condensation of a film on an inclined surface of width b. The assumptions used in the derivation are:

- The flow of liquid film is laminar,
- For liquid films, constant characteristics are assumed,
- At temperature $T_{sat,}$ the gas is pure vapour. Heat is transmitted to the liquid-vapour interface exclusively through interface condensation and conduction from the vapour,
- It is considered that the interface experiences insignificant shear stress, which means $\left.\frac{\partial u}{\partial y}\right|_{y=\delta} = 0$,
- Condensate film is considered to experience negligible momentum transfer as well as energy transfer due to advection.

In terms of the film, the equation representing the momentum in the *x*-direction can be expressed as [57]:

$$\frac{\partial^2 u}{\partial y^2} = \frac{g\sin\theta}{\mu_l}\left(\rho_l - \rho_v\right) \tag{7}$$

By double integration of the previous equation and imposing boundary conditions $u(0) = 0$ and $\left.\frac{\partial u}{\partial y}\right|_{y=\delta} = 0$, the velocity distribution of fluid within the film can be written as [57,58]:

$$u(y) = \frac{g\sin\theta}{\mu_l}\left(\rho_l - \rho_v\right)\delta^2\left[\frac{y}{\delta} - \frac{1}{2}\left(\frac{y}{\delta}\right)^2\right] \tag{8}$$

From the above result, the flow rate of condensed film per width, $\gamma(x)$, can be computed as [57]:

$$\gamma(x) = \frac{\dot{m}(x)\cos\theta}{\mu_l} = \int_0^{\delta(x)} \rho_l u(y)dy \tag{9}$$

From Eqn. (8) and Eqn. (9), $\gamma(x)$ can be expressed as [57]:

$$\gamma(x) = \frac{\rho_l\left(\rho_l - \rho_v\right)\delta^3 g\sin\theta}{3\mu_l} \tag{10}$$

The variation of δ and γ with respect to x can be derived by implementing the energy conservation for the small element of unit width and length dx, as illustrated in Figure 3. The heat flux rate directed into the film element, dq, must be balanced by the latent heat of condensation. Hence:

$$dq = h_{fg} \times d\dot{m} \times \cos\theta \tag{11}$$

From Eqn. (9) and Eqn. (11), one can get:

$$dq = h_{fg} \times b \times d\gamma \tag{12}$$

Due to insignificant advection, the interfacial heat transfer and heat transmission to the condensing cover must be equivalent. This refers to:

$$dq = q_s'' \times (b \times dx) \tag{13}$$

Heat flux at the surface due to the linear distribution of liquid temperature can be expressed using Fourier's law [38], which is defined as:

$$q_s'' = \frac{k_l(T_{sat} - T_s)}{\delta} \tag{14}$$

By merging Eqn. (12) and Eqn. (13) through Eqn. (14), one can get:

$$\frac{d\gamma}{dx} = \frac{k_l(T_{sat} - T_s)}{\delta \times h_{fg}} \tag{15}$$

By differentiating Eqn. (10), the expression of $d\gamma$ can also be written as:

$$\frac{d\gamma}{dx} = \frac{g\sin\theta\rho_l\left(\rho_l - \rho_v\right)\delta^2}{\mu_l}\frac{d\delta}{dx} \tag{16}$$

By combining Eqn. (15) and Eqn. (16), one can get:

$$\delta^3 d\delta = \frac{k_l \mu_l(T_{sat} - T_s)}{g\sin\theta\rho_l\left(\rho_l - \rho_v\right)h_{fg}}dx \tag{17}$$

By integrating the Eqn. (17) from zero to any desired position of *x*, the value of $\delta(x)$ becomes:

$$\delta(x) = \left[\frac{4k_l\mu_l(T_{sat} - T_s)x}{g\sin\theta\rho_l(\rho_l - \rho_v)h_{fg}}\right]^{\frac{1}{4}} \tag{18}$$

Brouwers [56] proposed a modified form of latent heat to account for the thermal advection effect.

$$h'_{fg} = h_{fg} + 0.68c_{p,l}\left(T_{sat} - T_s\right) \quad (19)$$

Sadasivan and Lienhard [39] have observed a correlation between the modified heat of transformation and the Prandtl number of the liquid. The rate of surface heat transmission can be derived as [39]:

$$h'_{fg} = h_x\left(T_{sat} - T_s\right) \quad (20)$$

From Eq. (14), the local heat convection coefficient is defined as:

$$h_x = \frac{kl}{\delta} \quad (21)$$

and from Eq. (18), local heat convection coefficient with modified latent heat h'_{fg} becomes:

$$h_x = \left[\frac{g\sin\theta\rho_l\left(\rho_l - \rho_v\right)k_l^3 h'_{fg}}{4\mu_l(T_{sat} - T_s)x}\right]^{\frac{1}{4}} \quad (22)$$

For the entire glass plate, the average convection coefficient is defined as:

$$\bar{h}_L = \frac{1}{L}\int_0^L h_x dx = \frac{4}{3}h_L \quad (23)$$

or

$$\bar{h}_L = 0.943\left[\frac{g\sin\theta\rho_l\left(\rho_l - \rho_v\right)k_l^3 h'_{fg}}{\mu_l(T_{sat} - T_S)L}\right]^{\frac{1}{4}} \quad (24)$$

The average Nusselt number can be expressed as:

$$\overline{Nu}_L = \frac{\bar{h}_L \times L}{k_l} = 0.943\left[\frac{g\sin\theta\rho_l\left(\rho_l - \rho_v\right)L^3 h'_{fg}}{\mu_l k_l(T_{sat} - T_S)}\right]^{\frac{1}{4}} \quad (25)$$

The overall surface heat transmission can be computed by utilizing Eqn. (24)

$$q = \bar{h}_L A\left(T_{sat} - T_s\right) \quad (26)$$

Hence, the total condensation rate (distillate output) can be derived utilizing the following relation:

$$\dot{m} = \frac{q}{h'_{fg}} = \frac{\bar{h}_L A\left(T_{sat} - T_s\right)}{h'_{fg}} \quad (27)$$

4. Observation, result, and discussions

The changes over time in the level of sun radiation and the ambient temperature are depicted in Figure 4. At the initial phase of the investigation (i.e., 9:00 h), the value of solar radiation measured was 416 W/m^2, and it increased to 1156 W/m^2 by 13:00 h. After that, at 19:00 h, it decreased and eventually reached 0 W/m^2. Similarly, the ambient temperature followed a comparable trend. At 9:00 h, when the experiment began, the ambient temperature was 12.3℃; after that, it rose and reached to its peak of 26.3℃ at 16:00 h. Following this peak, it gradually decreased to 9.5℃ at 32:00 h as solar radiation diminished.

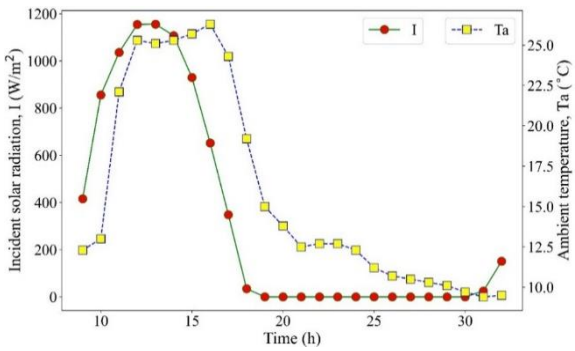

Figure 4. Variation in sun radiation and surrounding temperature over time

The changes over time in water surface temperature are represented in Figure 5. At the initial phase of the investigation (i.e., 9:00 h), the water temperature was 12.7℃, which increased with the rising intensity of solar energy. The apex of T_w was observed as 66.4℃ at 16:00 h, indicating maximum heat absorption under peak solar radiation. Following that, it decreased to a value of 9.6℃ at 32:00 h due to the diminution of solar radiation.

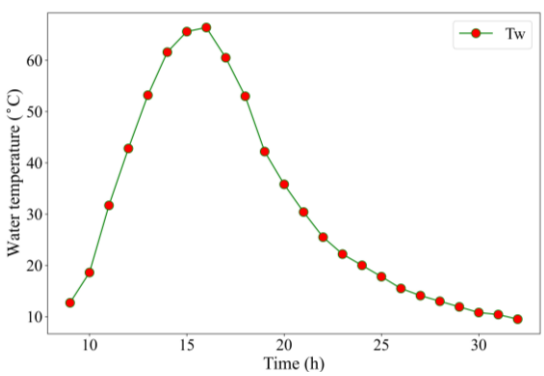

Figure 5. Variation in water surface temperature over time

Figure 6 depicts the changes over time in inner glass surface temperature. It has been noted that the inner glass surface temperature (T_{ci}) is more than the water surface temperature (T_w) at the commencement of the experiment. This is due to the fact that solar radiation only begins to reach the water surface after 8:00 h. The solar radiation that arrives first heats up

the condensing cover, after which the water gradually absorbs the heat. The water, having a greater heat capacity than the glass, takes a longer time to reach its elevated temperature. At 9:00 h, when the experiment began, the inside glass surface temperature was 12.9℃, after that, it rose and reached to its peak value of 45.8℃ at 15:00 h. Following this peak, the temperature gradually declined as solar radiation decreased. Thereafter, it decreased to a value of 8.2℃ at 32:00 h.

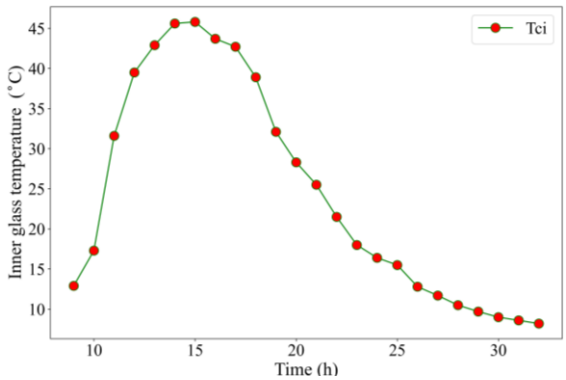

Figure 6. Variation in inner glass surface temperature over time

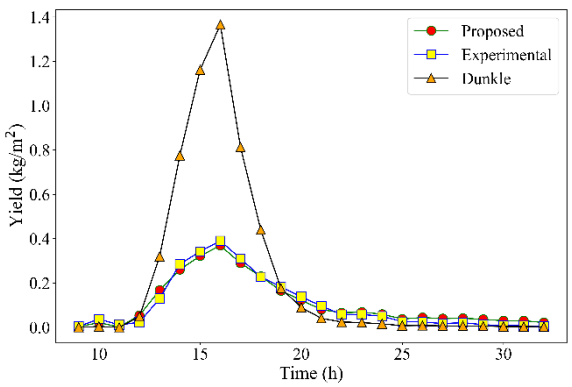

Figure 7. Variation in yield over time

The changes over time in distillate output are shown in Figure 7. It shows the comparative variation of the theoretical (Dunkle and Proposed) and experimental yields in one plot. From the initiation of the experiment (i.e., 9:00 h) till 11:00 h, the experimental yield leads over the Dunkle model. After 11:00 h, the Dunkle model predicts a much higher yield than the experimental results because it assumes idealized conditions, leading to an overestimation of the yield compared to real-world observations. This trend continues until 18:00 h. After 18:00 h, experimental yield takes its lead again over the Dunkle model and maintains it till the end.

At 16:00 h, the maximum value of yield from the Dunkle model is 1.365 kg/m^2, while the maximum experimental yield is 0.39 kg/m^2, i.e., the Dunkle model overestimates the result by 250.0% compared to the experimental value. This is due to the fact that the Dunkle model is only best fit when the average temperature range is 50℃ and the operational temperature range is 17℃. Moreover, the model is independent of cavity dimensions. At 16:00 h, the maximum value of yield from the proposed model is 0.36 kg/m^2, while the maximum experimental yield is 0.39 kg/m^2, i.e., the proposed model predicts 5.4% lower than the experimental yield.

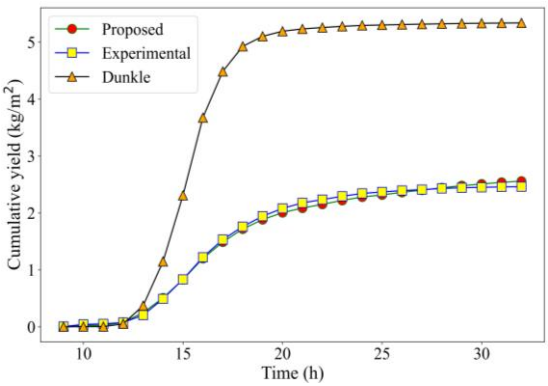

Figure 8. Variation in cumulative yield over time

The variations in cumulative distillate yield over time are depicted in Figure 8. The data compares three different yield predictions: the Dunkle model, the proposed model, and actual experimental results. The cumulative yields from the Dunkle model, proposed model, and experiment are 5.33, 2.46, and 2.56 kg/m^2, respectively. The Dunkle model predicts the highest cumulative yield as it is based on idealized conditions that do not fully consider real-world variables. This indicates that the Dunkle model predicts a distillate yield 116.8% higher than the experimental output, whereas the proposed model shows a deviation of only 4.0%.

5. Conclusions

The distillate output from CSS has been examined experimentally and theoretically at Guna (latitude: 24° 39′N, longitude: 77° 19′E), India, under weather conditions in the months of April and May 2024. To estimate the distillate production of CSS, a novel theoretical model based on the condensation rate has been proposed. The results obtained from both the experimental and theoretical analysis indicate that the proposed model yields a distillate output that closely

matches the experimental results, with a minimal deviation of only 4.0%, whereas the cumulative distillate output obtained from the Dunkle model deviates by 116.8%. Hence, it may be concluded that the proposed theory will estimate the distillate production of CSS accurately in comparison to a conventional predictive model.

Future research could focus on testing the proposed model under varying climatic conditions to evaluate its strength and adaptability. Also, combining the model with other modifications of CSS, such as thermal energy storage systems or advanced materials, could further enhance its performance and broaden its usability. These possibilities would provide valuable insights for optimizing solar still designs in different environmental conditions.

Acknowledgements

The authors thank Mr. Saksham Sharma and Mr. Harshit Gautam for assisting us during the experiments.

Nomenclature

A	area of condensing cover (m^2)
a_1	accuracy of equipment
A_s	surface area of basin of still (m^2)
b	width of condensing cover (m)
C	Constant
$c_{p,l}$	liquid's specific heat at constant pressure (J/kg-k)
d	characteristic dimension of still (m)
g	acceleration due to gravity (m/sec^2)
Gr	Grashof number
h'_{fg}	modified latent heat (J/kg)
h_{cw}	coefficient of convective heat transfer from water to condensing surface (W/m^2-K)
h_{ew}	coefficient of evaporative heat transfer from water to condensing surface (W/m^2-K)
h_{fg}	latent heat of vaporization (J/kg)
h_L	coefficient of mean convection (W/m^2-K)
h_x	coefficient of local convection (W/m^2-K)
I	solar radiation on condensing surface (W/m^2)
k	heat-conducting capacity of moist air (W/m-K)
L	length of condensing cover (m)
$\dot{m}$	total condensation rate (kg/sec)
$\dot{m}(x)$	condensation mass flow rate at the location x (kg/sec)
$\dot{m}_{ew}$	distillate production (kg/m^2-h)
n	Constant
Nu	Nusselt number
P_{ci}	pressure of the vapor in a saturated state on the inner condensing surface (Pa)
P_w	pressure of the vapor in a saturated state on water surface (Pa)
Pr	Prandtl number
q	overall heat transfer (W)
q''_s	surface heat flux (W/m^2)
Ra	Rayleigh number
T_a	atmospheric temperature (℃)
T_{ci}	temperature of the inner surface of condensing cover (℃)
T_s	temperature at inner surface of condensing cover (℃)
T_{sat}	saturation temperature of thermal boundary layer (℃)
T_w	temperature of the surface of the water (℃)
$u(y)$	fluid velocity profile at the location y (m/sec)
u_1	standard uncertainty
Greek Letter	
$\delta(x)$	boundary layer thickness at the location x (m)
θ	condensing cover inclination (º)
k_l	heat-conducting conductivity of liquid (W/m-k)
μ_l	dynamic viscosity (kg/m-s)
ρ_l	liquid's density (kg/m^3)
ρ_v	vapour's density (kg/m^3)
Abbreviations	
CSS	conventional solar still
FRP	fiber reinforced plastic

References

[1] G.N. Tiwari, A.K. Tiwari, Solar Distillation Practice for Water Desalination Systems, Anamaya, New Delhi, India, 2008. ISBN:

8188342718.
[2] A.E. Kabeel, S.A. El-Agouz, Review of researches and developments on solar stills, Desalination 276 (2011) 1–12. https://doi.org/10.1016/j.desal.2011.03.042.
[3] G.M. Ayoub, L. Malaeb, Developments in solar still desalination systems: A critical review, Crit. Rev. Environ. Sci. Technol. 42 (2012) 2078–2112. https://doi.org/10.1080/10643389.2011.574104.
[4] P. Prakash, V. Velmurugan, Parameters influencing the productivity of solar stills – A review, Renew. Sustain. Energy Rev. 49 (2015) 585–609. https://doi.org/10.1016/j.rser.2015.04.136.
[5] H. Panchal, I. Mohan, Various methods applied to solar still for enhancement of distillate output, Desalination 415 (2017) 76–89. https://doi.org/10.1016/J.DESAL.2017.04.015.
[6] H. Panchal, N. Patel, H. Thakkar, Various techniques for improvement in distillate output from active solar still: a review, Int. J. Ambient Energy 38 (2017) 209–222. https://doi.org/10.1080/01430750.2015.1076518.
[7] D. Mevada, H. Panchal, K. kumar Sadasivuni, M. Israr, M. Suresh, S. Dharaskar, H. Thakkar, Effect of fin configuration parameters on performance of solar still: A review, Groundw. Sustain. Dev. 10 (2020) 100289. https://doi.org/10.1016/j.gsd.2019.100289.
[8] H. Panchal, K. Patel, M. Elkelawy, H.A.-E. Bastawissi, A use of various phase change materials on the performance of solar still: a review, Int. J. Ambient Energy 0 (2019) 1–6. https://doi.org/10.1080/01430750.2019.1594376.
[9] A.K. Tiwari, G.N. Tiwari, Effect of water depths on heat and mass transfer in a passive solar still: in summer climatic condition, Desalination 195 (2006) 78–94. https://doi.org/10.1016/j.desal.2005.11.014.
[10] B. Jamil, N. Akhtar, Effect of specific height on the performance of a single slope solar still: An experimental study, Desalination 414 (2017) 73–88. https://doi.org/10.1016/j.desal.2017.03.036.
[11] M. Afrand, A. Karimipour, Theoretical analysis of various climatic parameter effects on performance of a basin solar still, J. Power Technol. 97 (2017) 44–51. https://api.semanticscholar.org/CorpusID:55109734.
[12] P. Dumka, D.R. Mishra, Influence of salt concentration on the performance characteristics of passive solar still, Int. J. Ambient Energy (2019) 1–11. https://doi.org/10.1080/01430750.2019.1611638.
[13] P. Dumka, D.R. Mishra, Energy and exergy analysis of conventional and modified solar still integrated with sand bed earth: Study of heat and mass transfer, Desalination 437 (2018) 15–25. https://doi.org/10.1016/j.desal.2018.02.026.
[14] P. Dumka, D.R. Mishra, Experimental investigation of modified single slope solar still integrated with earth (I) {\&} (II):Energy and exergy analysis, Energy 160 (2018) 1144–1157. https://doi.org/10.1016/J.ENERGY.2018.07.083.
[15] T. Arunkumar, A.E. Kabeel, K. Raj, D. Denkenberger, R. Sathyamurthy, P. Ragupathy, R. Velraj, Productivity enhancement of solar still by using porous absorber with bubble-wrap insulation, J. Clean. Prod. 195 (2018) 1149–1161. https://doi.org/10.1016/j.jclepro.2018.05.199.
[16] A.E.E. Kabeel, W.M. El-maghlany, Y.A.F. El-Samadony, W.M. El-maghlany, Comparative study on the solar still performance utilizing different PCM, Desalination 432 (2018) 89–96. https://doi.org/10.1016/J.DESAL.2018.01.016.
[17] A.E. Kabeel, S.A. El-agouz, R. Sathyamurthy, T. Arunkumar, Augmenting the productivity of solar still using jute cloth knitted with sand heat energy storage, Desalination 443 (2018) 122–129. https://doi.org/10.1016/j.desal.2018.05.026.
[18] D.R. Mishra, A.K. Tiwari, Effect of coal and metal chip on the solar still, J. Sci. Tech. Res. 3 (2013) 1–6. ISSN: 2278-3350.
[19] K. Khanafer, K. Vafai, A review on the applications of nanofluids in solar energy field, Renew. Energy 123 (2018) 398–406. https://doi.org/10.1016/j.renene.2018.01.097.
[20] H.S. Deshmukh, S.B. Thombre, Solar distillation with single basin solar still using sensible heat storage materials, Desalination

410 (2017) 91–98. https://doi.org/10.1016/j.desal.2017.01.030.

[21] P. Dumka, Y. Kushwah, A. Sharma, D.R. Mishra, Comparative analysis and experimental evaluation of single slope solar still augmented with permanent magnets and conventional solar still, Desalination 459 (2019). https://doi.org/10.1016/j.desal.2019.02.012.

[22] T. Rajaseenivasan, R. Prakash, K. Vijayakumar, K. Srithar, Mathematical and experimental investigation on the influence of basin height variation and stirring of water by solar PV panels in solar still, Desalination 415 (2017) 67–75. https://doi.org/10.1016/j.desal.2017.04.010.

[23] Z.M. Omara, A.S. Abdullah, T. Dakrory, Improving the productivity of solar still by using water fan and wind turbine, Sol. Energy 147 (2017) 181–188. https://doi.org/10.1016/j.solener.2017.03.041.

[24] A.E. Kabeel, R. Sathyamurthy, S.W. Sharshir, A. Muthumanokar, H. Panchal, N. Prakash, C. Prasad, S. Nandakumar, M.S. El Kady, Effect of water depth on a novel absorber plate of pyramid solar still coated with TiO 2 nano black paint, J. Clean. Prod. 213 (2019) 185–191. https://doi.org/10.1016/j.jclepro.2018.12.185.

[25] P. Dumka, D.R. Mishra, Performance evaluation of single slope solar still augmented with the ultrasonic fogger, Energy 190 (2020). https://doi.org/10.1016/j.energy.2019.116398.

[26] R. Kumar, D.R. Mishra, P. Dumka, Improving solar still performance : A comparative analysis of conventional and honeycomb pad augmented solar stills, 270 (2024). https://doi.org/10.1016/j.solener.2024.112408.

[27] P. Dumka, N. Pandey, D.R. Mishra, Journal of Solar Energy Research (JSER) Conventional Solar Still Augmented with Saltwater Bottles : An Experimental Study, 9 (2024) 1811–1821. https://doi.org/10.22059/jser.2024.374131.1392.

[28] S. Shoeibi, F. Jamil, S.M. Parsa, S. Mehdi, H. Kargarsharifabad, S.A.A. Mirjalily, W. Guo, H.H. Ngo, B.-J. Ni, M. Khiadani, Recent advancements in applications of encapsulated phase change materials for solar energy systems: A state of the art review, J. Energy Storage 94 (2024) 112401. https://doi.org/10.1016/j.est.2024.112401.

[29] S. Shoeibi, H. Kargarsharifabad, M. Khiadani, S.M. Parsa, S.A.A. Mirjalily, H.A. Mohammed, Techniques used to enhance condensation rate of solar desalination systems: State-of-the-art review, Int. Commun. Heat Mass Transf. 159 (2024) 108164. https://doi.org/10.1016/j.icheatmasstransfer.2024.108164.

[30] A. Hemmatian, H. Kargarsharifabad, A. Abedini Esfahlani, N. Rahbar, S. Shoeibi, Improving solar still performance with heat pipe/pulsating heat pipe evacuated tube solar collectors and PCM: An experimental and environmental analysis, Sol. Energy 269 (2024) 112371. https://doi.org/10.1016/j.solener.2024.112371.

[31] B. Khalili, H. Kargarsharifabad, N. Rahbar, A. Abedini Esfahlani, E. Jamshidi, Performance evaluation of a CGS gas heater-powered HDH desalination system using thermosyphon heat pipes: An experimental study with economic and environmental assessment, Int. Commun. Heat Mass Transf. 152 (2024) 107300. https://doi.org/10.1016/j.icheatmasstransfer.2024.107300.

[32] H.K.M.S.A.A. Ramasamy Dhivagar Shahin Shoeibi, M. Khiadani, Performance analysis of solar desalination using crushed granite stone as an energy storage material and the integration of solar district heating, Energy Sources, Part A Recover. Util. Environ. Eff. 46 (2024) 1370–1388. https://doi.org/10.1080/15567036.2023.2299693.

[33] W.A. Abdelmaksoud, Enhancing water productivity of solar still using thermal energy storage material and flat plate solar collector, Appl. Water Sci. 15 (2025). https://doi.org/10.1007/s13201-024-02340-x.

[34] M.P.R. Teles, M. Sadi, K.A.R. Ismail, A. Arabkoohsar, B.V.F. Silva, H. Kargarsharifabad, S. Shoeibi, Cooling supply with a new type of evacuated solar collectors: a techno-economic optimization and analysis, Environ. Sci. Pollut. Res. 31 (2024) 18171–

18187. https://doi.org/10.1007/s11356-023-25715-0.

[35] M. Bhargva, M. Sharma, A. Yadav, N.K. Batra, R.K. Behl, Productivity Augmentation of a Solar Still with Rectangular Fins and Bamboo Cotton Wick, J. Sol. Energy Res. 8 (2023) 1410–1416. https://doi.org/10.22059/jser.2023.356414.1279.

[36] A. Farzi, R. Nameni, H. Asadollahi, Enhancement of single slope solar still using sand : the effect of sand grain size distribution, J. Sol. Energy Res. 6 (2021) 740–750. https://doi.org/10.22059/jser.2021.320642.1194.

[37] M. Gholizadeh, A. Farzi, Performance Improvement of the single slope Solar Still Using Sand, J. Sol. Energy Res. 5 (2020) 560–567. https://doi.org/10.22059/jser.2020.302120.1152.

[38] S. Ahmed, K. Mohammad, S. Bhuiya, P. Das, A. Shahriyar, A. Haque, Z. Tasnim, M. Jahan, Journal of Solar Energy Research (JSER) Advancements in Solar Still Water Desalination : A Comprehensive Review of Design Enhancements and Performance Optimization, 9 (2025) 2025–2061. https://doi.org/10.22059/jser.2025.382301.1464.

[39] S.A. Alamshah, M. Talebzadegan, M. Moravej, Performance Evaluation of Regular Hexagonal Pyramid Three-Dimensional Solar Desalination System: An Experimental Investigation, J. Sol. Energy Res. 9 (2024) 1914–1925. https://doi.org/10.22059/jser.2024.370071.1371.

[40] R.K. Das, A. Date, Sustainable water desalination using eductor and waste heat : A review and suggestion for future research, 603 (2025). https://doi.org/10.1016/j.desal.2025.118687.

[41] M. El-Sayed M. Essa, H.S. El-sayed, E.E. El-kholy, M. Amer, M. Elsisi, U. Sajjad, K. Hamid, H. El-sayed Awad, Developments in solar-driven desalination: Technologies, photovoltaic integration, and processes, Energy Convers. Manag. X 25 (2025). https://doi.org/10.1016/j.ecmx.2024.100861.

[42] R. V Dunkle, Solar water distillation: the roof type still and a multiple effect diffusion still, in: Int. Dev. Heat Transf. ASME, Proc. Int. Heat Transf. Part V, Univ. Color., 1961: pp. 895–902.

[43] P.I. Cooper, Digital simulation of transient solar still processes, Sol. Energy 12 (1969) 313–331. https://doi.org/10.1016/0038-092X(69)90046-2.

[44] P.I. Cooper, The maximum efficiency of single-effect solar stills, Sol. Energy 15 (1973). https://doi.org/10.1016/0038-092X(73)90085-6.

[45] B. Frick, Some new considerations about solar stills, in: Proc. Int. J. Sol. Energy, Melbourne, 1970: p. 395.

[46] N.J. K., G.N. Tiwari, M.S. Sodha, PERIODIC THEORY OF SOLAR STILL, 4 (1980) 41–57. https://doi.org/10.1002/er.4440040106.

[47] M.S. Sodha, U. Singh, A. Kumar, G.N. Tiwari, Transient analysis of solar still, Energy Convers. Manag. 20 (1980) 191–195. https://doi.org/10.1016/0196-8904(80)90033-3.

[48] W.A. Kamal, A theoretical and experimental study of the basin-type solar still under the arabian gulf climatic conditions, Sol. Wind Technol. 5 (1988) 147–157. https://doi.org/10.1016/0741-983X(88)90074-4.

[49] S. Kumar, G.N. Tiwari, Estimation of convective mass transfer in solar distillation systems, Sol. Energy 57 (1996) 459–464. https://doi.org/10.1016/S0038-092X(96)00122-3.

[50] P.T. Tsilingiris, The application and experimental validation of a heat and mass transfer analogy model for the prediction of mass transfer in solar distillation systems, Appl. Therm. Eng. 50 (2013) 422–428. https://doi.org/10.1016/j.applthermaleng.2012.07.007.

[51] T. Kiatsiriroat, S.C. Bhattacharya, P. Wibulswas, Prediction of mass transfer rates in solar stills, Energy 11 (1986) 881–886. https://doi.org/10.1016/0360-5442(86)90007-1.

[52] J.A. Clark, The steady-state performance of a solar still, Sol. Energy 44 (1990) 43–49. https://doi.org/10.1016/0038-092X(90)90025-8.

[53] D. B. Spalding, Convective Mass Transfer, Arnold, London, 1963.

[54] G.N. Tiwari, A. Tiwari, Shyam, Solar Distillation, Pergamon, Oxford, U.K, UK, 2016. https://doi.org/10.1007/978-981-10-

0807-8_13.

[55] J.A. Esfahani, N. Rahbar, M. Lavvaf, Utilization of thermoelectric cooling in a portable active solar still - An experimental study on winter days, Desalination 269 (2011) 198–205. https://doi.org/10.1016/j.desal.2010.10.062.

[56] H.J.H. Brouwers, Film condensation on non-isothermal vertical plates, Int. J. Heat Mass Transf. 32 (1989) 655–663. https://doi.org/10.1016/0017-9310(89)90213-5.

[57] T.L. Bergman, A.S. Lavine, F.P. Incropera, D.P. DeWitt, Fundamentals of Heat and Mass Transfer, 8th ed., John Wiley & Sons, Hoboken, NJ, 2018. https://doi.org/10.1016/j.applthermaleng.2011.03.022.

[58] G. Biswas, S.K. Som, Introduction to Fluid Mechanics and Fluid Machines, Tata McGraw-Hill Education, 2003. ISBN: 0070702594, 9780070702592.